

## **Supporting Information**

**Sandwich-like Co<sub>3</sub>O<sub>4</sub>/MXene composites as high capacity electrodes for lithium-ion batteries**

*Zeting Zhang, Huinan Guo, Weiqin Li, Guishu Liu, Yan Zhang, Yijing Wang\**

### **Contents**

**Figure S1**

**Figure S2**

**Figure S3**

**Figure S4**

**Figure S5**

**Figure S6**

**Figure S7**

**Figure S8**

**Figure S9**

**Figure S10**

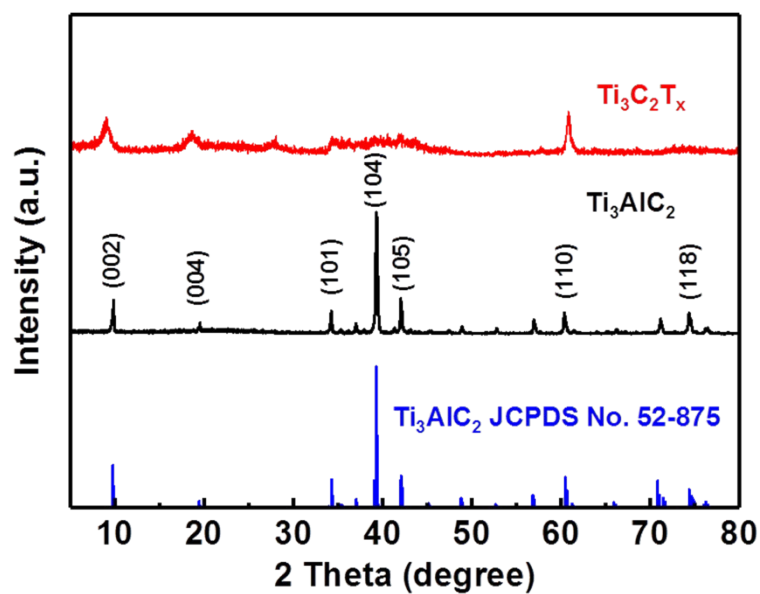


**Figure S1.** X-ray diffraction of  $\text{Ti}_3\text{C}_2\text{T}_x$  and  $\text{Ti}_3\text{AlC}_2$ .

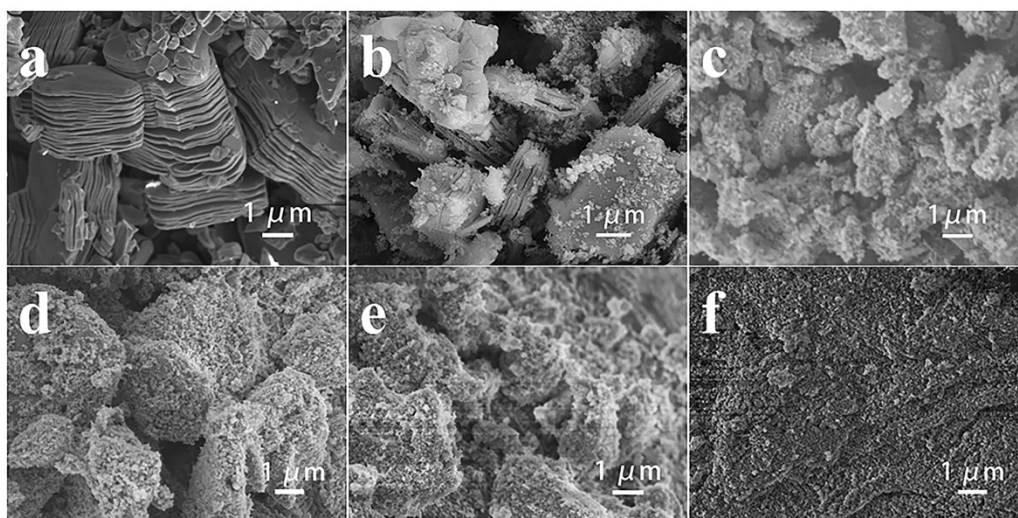


**Figure S2.** Low-resolution SEM images of (a)  $\text{Ti}_3\text{C}_2\text{T}_x$ , (b)  $\text{Co}_3\text{O}_4/\text{Ti}_3\text{C}_2\text{T}_x$ -1, (c)  $\text{Co}_3\text{O}_4/\text{Ti}_3\text{C}_2\text{T}_x$ -2, (d)  $\text{Co}_3\text{O}_4/\text{Ti}_3\text{C}_2\text{T}_x$ -3, (e)  $\text{Co}_3\text{O}_4/\text{Ti}_3\text{C}_2\text{T}_x$ -4 and (f)  $\text{Co}_3\text{O}_4$ .

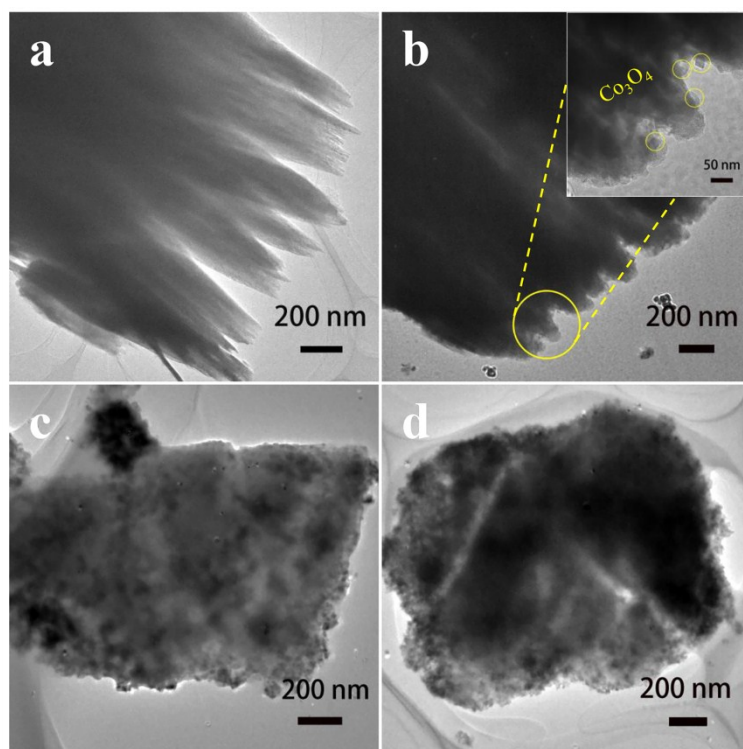


**Figure S3.** TEM images of (a)  $\text{Ti}_3\text{C}_2\text{T}_x$ , (b)  $\text{Co}_3\text{O}_4/\text{Ti}_3\text{C}_2\text{T}_x\text{-2}$ , (c)  $\text{Co}_3\text{O}_4/\text{Ti}_3\text{C}_2\text{T}_x\text{-3}$  and (d)  $\text{Co}_3\text{O}_4/\text{Ti}_3\text{C}_2\text{T}_x\text{-4}$ .

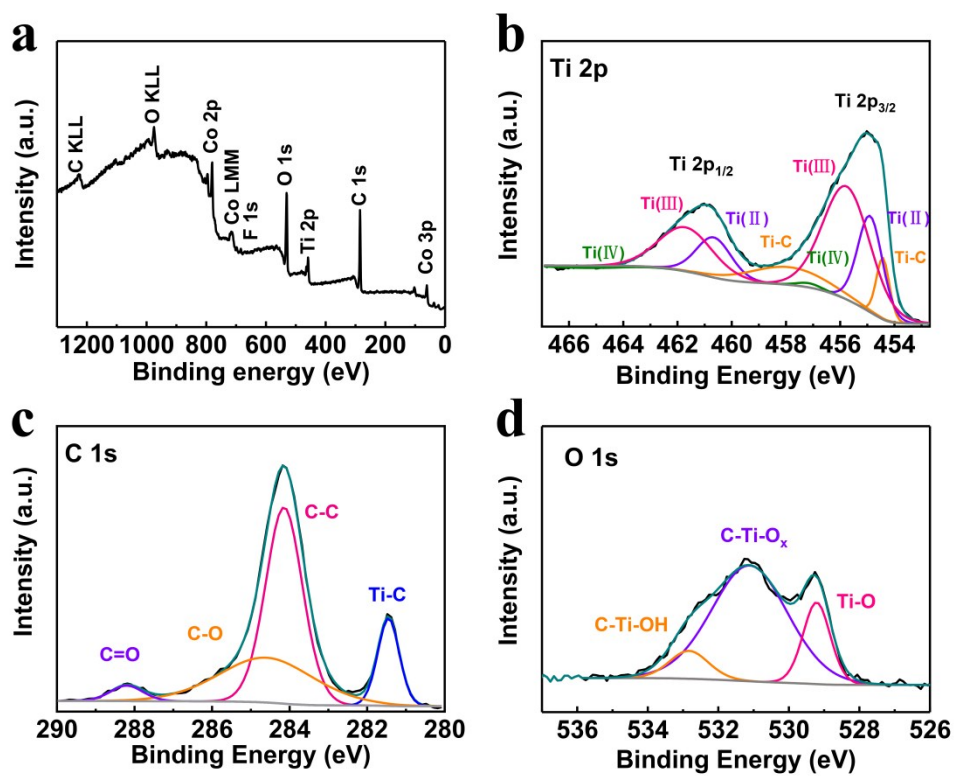


**Figure S4.** (a) XPS wide spectra of  $\text{Co}_3\text{O}_4/\text{Ti}_3\text{C}_2\text{T}_x$ -3. XPS fine spectra of (b) Ti, (c) C and (d) O for  $\text{Ti}_3\text{C}_2\text{T}_x$ .

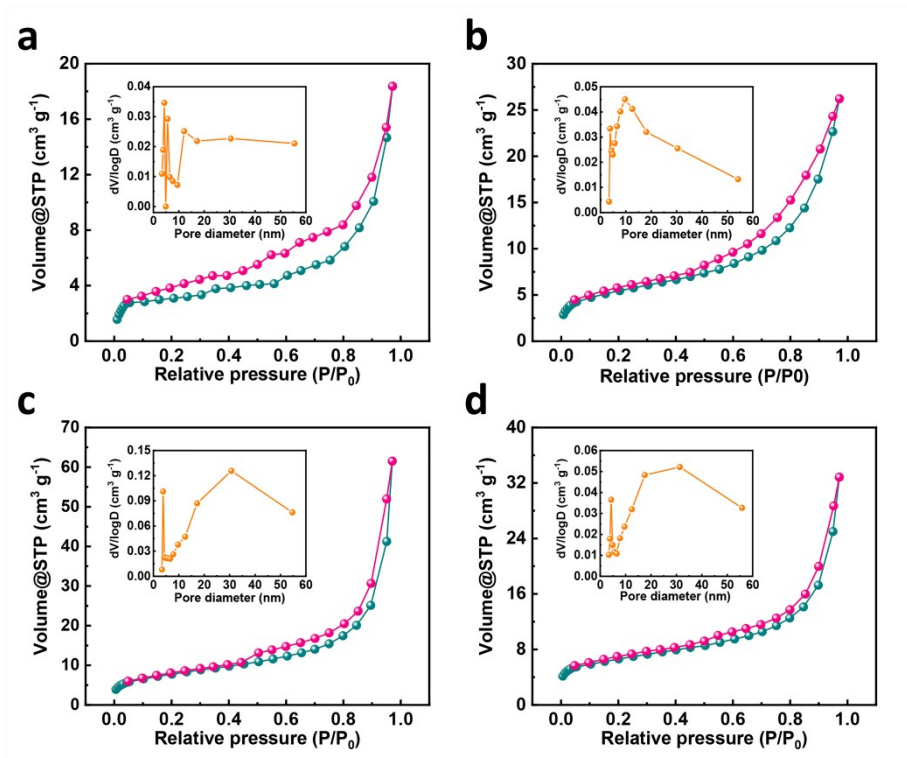


**Figure S5.** Nitrogen adsorption/desorption isotherms (pink: nitrogen adsorption curve; dark cyan: nitrogen desorption curve) and pore diameter distribution (inset) of (a)  $\text{Co}_3\text{O}_4/\text{Ti}_3\text{C}_2\text{T}_x$ -1, (b)  $\text{Co}_3\text{O}_4/\text{Ti}_3\text{C}_2\text{T}_x$ -2, (c)  $\text{Co}_3\text{O}_4/\text{Ti}_3\text{C}_2\text{T}_x$ -3 and (d)  $\text{Co}_3\text{O}_4/\text{Ti}_3\text{C}_2\text{T}_x$ -4.

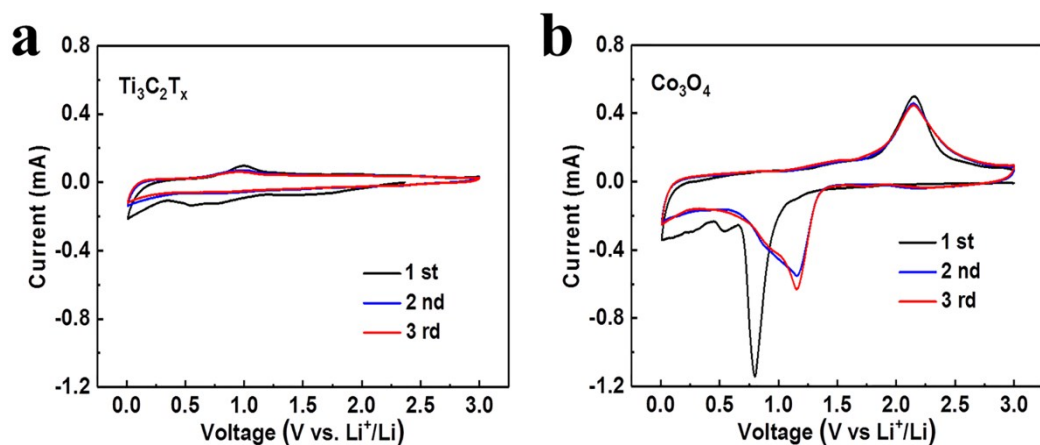


**Figure S6.** CV curves at  $0.5 \text{ mV s}^{-1}$  from 0.01 to 3 V of (a)  $\text{Ti}_3\text{C}_2\text{T}_x$  and (b)  $\text{Co}_3\text{O}_4$ .

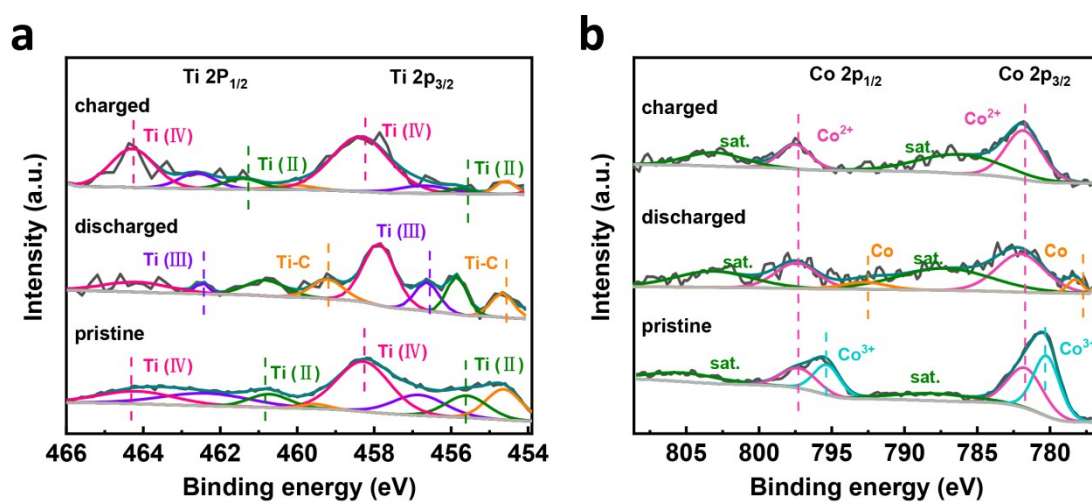


**Figure S7.** XPS fine spectra of (a) Ti, (b) Co of  $\text{Co}_3\text{O}_4/\text{Ti}_3\text{C}_2\text{T}_x$ -3 electrodes at pristine, fully discharged, and fully charged states.

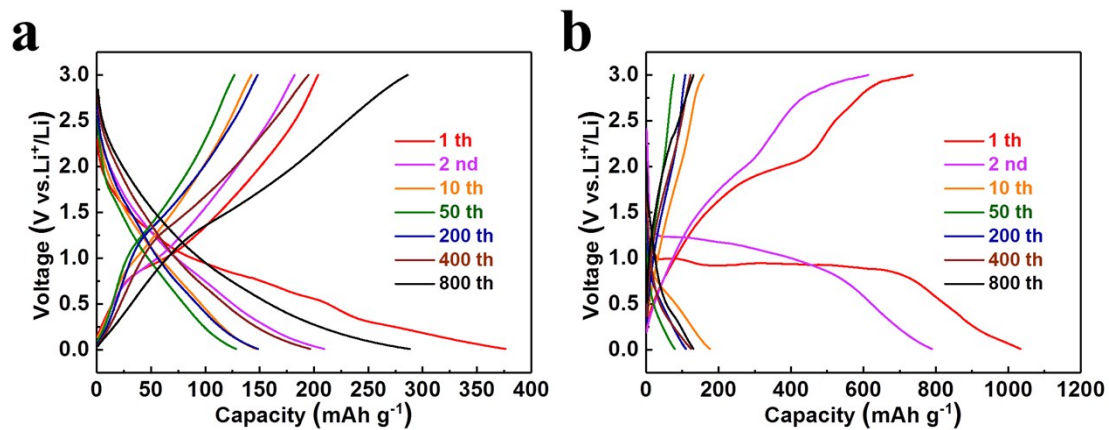


**Figure S8.** Galvanostatic charge-discharge curves at different cycles of (a)  $\text{Ti}_3\text{C}_2\text{T}_x$  and (b)  $\text{Co}_3\text{O}_4$  at  $500 \text{ mA g}^{-1}$ .

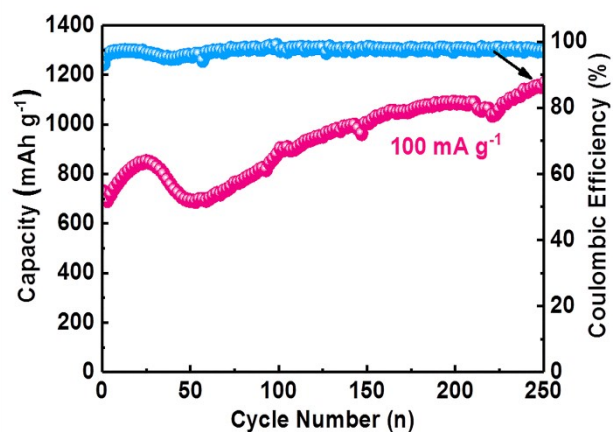


**Figure S9.** Cycling performance at  $100 \text{ mA g}^{-1}$  and coulombic efficiency of  $\text{Co}_3\text{O}_4/\text{Ti}_3\text{C}_2\text{T}_x\text{-3}$ .



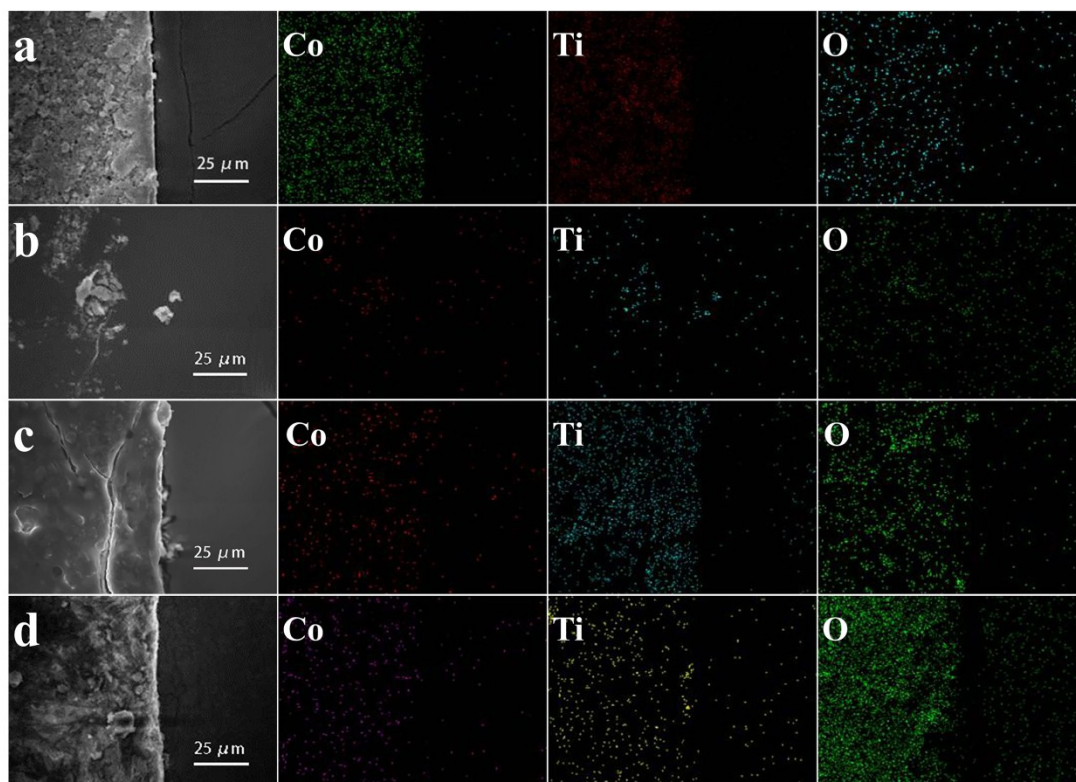


**Figure S10.** SEM images and corresponding elemental mappings of  $\text{Co}_3\text{O}_4/\text{Ti}_3\text{C}_2\text{T}_x-3$  electrodes at initial (a) and after (b) 50, (c) 300 and (d) 900 cycles.